

Adaptive 3D Radial MRI Based on Multidimensional Golden Means for Supine Breast Imaging

P. Siegler¹, R. W-C. Chan², E. A. Ramsay¹, and D. B. Plewes¹

¹Imaging Research, Sunnybrook Health Sciences Centre, Toronto, Ontario, Canada, ²Department of Medical Biophysics, University of Toronto, Toronto, Ontario, Canada

INTRODUCTION

Supine breast MRI [1] allows imaging of the breast in a configuration similar to many clinical applications including ultrasound and breast conserving surgeries. This would facilitate the image registration of MR images for aid of these applications. However, standard Cartesian sampling has non-isotropic spatial resolution, which is undesirable when the registered images are presented in various slice orientations.

Adaptive sampling of k -space allows the reconstruction of images with various spatial and temporal resolutions from the same data set and is therefore suitable for dynamic MRI [2,3]. Golden-angle radial k -space sampling achieves this flexibility in-plane with relatively uniform angular sampling distribution for any time interval using samples incremented by the golden angle [4]. To achieve a similar sampling pattern in 3D k -space with isotropic spatial resolution, this has been extended to 3D projection reconstruction (PR) based on multidimensional golden means ("golden 3D-PR") [5]. The uniform sampling of k -space over time with 2D radial MRI, can be combined with the k -space-weighted image contrast (KWIC) technique [6] to compensate for respiratory motion [7].

In this work, the golden 3D-PR was tested for use in supine breast MRI. The main focus was the compensation of respiratory motion, which is intrinsic if the patient is in a supine position during the scan.

MATERIALS AND METHODS

All experiments were performed on a whole body 1.5T MR scanner (GE Signa Excite) using a previously described setup for supine breast MRI [1]. A fast 3D spoiled gradient echo (fast 3D SPGR) sequence was modified for golden 3D-PR [4].

For motion-compensation during image-reconstruction, the respiration pattern was tracked during the scan using a respiratory belt. Two motion-compensation options were considered during the image-reconstruction: (a) k -space was filled in spherical shells (Fig 1), with projections having higher detected displacements being placed further from the centre ("post-processed reordering"). (b) Projections acquired during high displacement values were excluded from the image-reconstruction ("post-processed gating").

• Phantom experiments:

A high-resolution phantom was scanned ($\alpha=30^\circ$, BW=31.25kHz, FOV = 216×216×216mm³, $T_E=3.6$ ms, $T_R=10.0$ ms) without motion and then with periodical motion. From the moving phantom data, images were reconstructed without motion compensation, and with post-processed reordering and gating. In addition, the moving phantom was scanned using "acquisition gating", where data were rejected during the data-acquisition if the displacement exceeded a chosen threshold (75% of whole displacement range).

In order to achieve a chosen scan-time of 20s, the number of projections used for image reconstruction was varied. To increase the SNR, 8 images reconstructed from the isotropic 3D data-sets were combined to form images with a slice thickness of 6.75mm.

• Volunteer experiments:

A human volunteer was scanned after consent during free-breathing ($\alpha=30^\circ$, BW=31.25kHz, FOV = 252×252×252mm³, $T_E=3.5$ ms, $T_R=9.2$ ms). Images were reconstructed without motion-compensation and with post-processed reordering for a chosen scan-time of 102s (10,000 projections). To increase SNR, 8 images reconstructed from the isotropic 3D data-sets were combined to form images with a slice thickness of 6.75mm in axial and coronal slice-orientation.

RESULTS

The results of the phantom experiment (Fig. 2) demonstrate that post-processed reordering (Fig. 2c) achieves some degree of compensation for periodic motion artifacts. Both gating methods achieve comparable motion-compensation results (Fig. 2d,e). However, post-processed gating does not require the gating limit to be chosen prior the scan.

In the volunteer experiment, the image quality could be increased using post-processed reordering (see arrows in Fig. 3a,c and Fig. 3b,d). The isotropic spatial resolution of the golden 3D-PR allows the presentation of images in various slice orientations with the same in-plane spatial resolution.

DISCUSSION AND CONCLUSIONS

Golden 3D-PR allows post-processed compensation for respiratory motion without the need to choose any motion-compensation settings prior to the scan. The isotropic spatial resolution and the flexibility to reconstruct various spatial and temporal resolutions from the same data set make golden 3D-PR very useful for supine breast MRI for later image-aided applications.

REFERENCES

[1] Siegler P, et al. Proc ISMRM 2009:2112 [2] Rasche V, et al. MRM 1995;34:754-61 [3] Peters DC, et al. MRM 2000;43:91-101 [4] Winkelmann S, et al. IEEE TMI 2007;26:68-76 [5] Chan RWC, et al. MRM 2008 in press [6] Song HK, et al. MRM 2004;52:815-24 [7] Lin W, et al. MRM 2008;60:1135-46

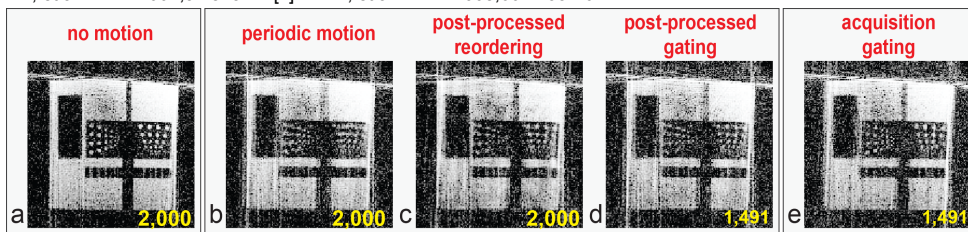


Figure 2: Images of the high-resolution phantom. (a) Without motion. (b) With uncompensated periodic motion (c) With motion with post-processed reordering and (d) post-processed gating. (e) Acquisition gating. A fixed scan time of 20s was achieved by varying the number of projections (right corner of each image) used for reconstruction.

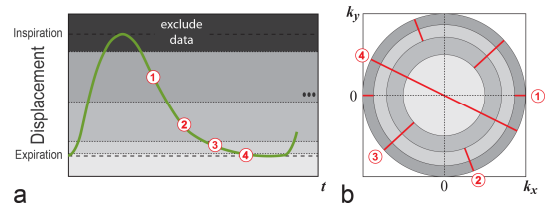


Figure 1: Post-processed motion-compensation (for simplicity shown in 2D with four zones: (a) Segmentation of the displacement. (b) Filling of the k -space with the projections depending on the tracked displacement.

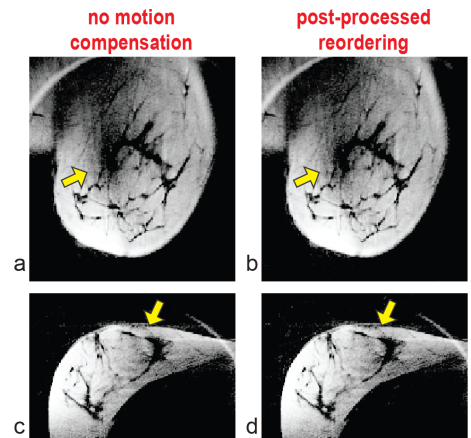


Figure 3: Slices through a 3D-PR-data-set reconstructed (10,000 projections) without motion compensation and with post-processed reordering. (a)/(b) in a coronal and (c)/(d) in axial slice orientation. The arrows indicate regions with increased image quality due to motion compensation.